α-D-Cellooligosaccharide Acetates: Physical and Spectroscopic Characterization and Evaluation as Models for Cellulose Triacetate

Charles M. Buchanan,* John A. Hyatt,* Stephen S. Kelley, and James L. Little

Research Laboratories, Eastman Chemical Company, P.O. Box 1972, Kingsport, Tennessee 37662

Received October 25, 1989; Revised Manuscript Received February 13, 1990

ABSTRACT: The series of crystalline oligomers from α-D-cellobiose octaacetate through α-D-cellononaose nonacosaacetate was prepared and characterized by mass spectrometry, by ^1H and ^{13}C NMR spectroscopy, and by differential scanning calorimetry. Through extrapolation of these values to cellulose triacetate (CTA), the resulting data are discussed in terms of the critical degree of polymerization (DP). Carbon-13 spin–lattice relaxation values (T_1) indicate a critical DP of 7; it is predicted that the T_m and H_f of CTA should be 294 °C and 4.9 kcal/mol. These values are discussed in relation to experimental values for CTA. Complete ^1H and ^{13}C NMR assignments and a protocol for obtaining useful mass spectra via positive-ion liquid secondary ion mass spectrometry (LSIMS) for cellooligosaccharide acetates are provided.

Cellulose derivatives are unique among commercially important plastic materials in that their polymer backbone is both biodegradable and derived from renewable resources. But despite many decades' production, use, and study, the structure–property relationships, crystallization behavior, conformational properties, and molecular dynamics of cellulose triacetate (CTA (1)) and related cellulosic materials are poorly understood when compared to many synthetic polymers.[1]

It is possible to gain an understanding of many polymer properties by examining a homologous series of oligomeric compounds that asymptotically approach the polymer structure. Thus in the polysaccharide area, Benesi and Brant[2] have reported the use of ^{13}C nuclear magnetic resonance (NMR) dipolar relaxation and nuclear Overhauser effect (NOE) values as tools for comparing a series of pullulan and maltooligosaccharide oligomers and polymers. These NMR techniques allowed them to compare molecular motion in low and high molecular weight regions and to define a critical degree of polymerization (DP) of 15 for pullulan (i.e., the DP at which segmental motion begins to dominate and above which the NMR relaxation parameters are independent of molecular weight).

Prompted by our own interest in the chemistry of cellulose esters,[3-5] we have elected to follow an approach similar to that of Benesi and Brant.[2] For the series of crystalline oligomers α-D-cellobiose octaacetate (**2**) through α-D-cellononaose nonacosaacetate (**9**), we report values for melting point (T_m), heat of fusion (H_f), ^1H and ^{13}C NMR assignments, and ^{13}C T_1 relaxation times. These data are compared to those of CTA (**1**), and attempts are made to determine, for various physical characteristics, at what size a cellooligosaccharide acetate begins to behave like cellulose triacetate. In addition, we report the characterization of the heretofore unreported α-D-cellooctaose and α-D-cellononaose acetates, including a mass spectroscopic protocol for obtaining molecular ions and specific fragmentation of the higher cellooligosaccharide acetates.

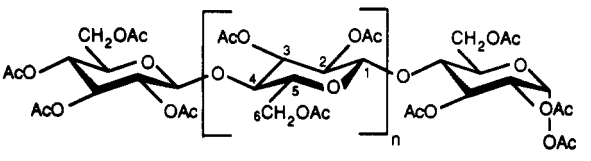

n = 0, Cellobiose Octaacetate (2)
n = 1, Cellotriose Hendecaacetate (3)
n = 2, Cellotetraose Tetradecaacetate (4)
n = 3, Cellopentaose Heptadecaacetate (5)
n = 4, Cellohexaose Eicosaacetate (6)
n = 5, Celloheptaose Tricosaacetate (7)
n = 6, Cellooctaose Hexacosaacetate (8)
n = 7, Cellononaose Nonacosaacetate (9)
n > 50, Cellulose Triacetate (1)

Results and Discussion

Materials. The α-D-cellooligosaccharide acetates **2–9** were prepared by acetolysis of cellulose followed by chromatographic separation according to the general methods of Wolfrom and co-workers.[6-8] All oligomers were recrystallized twice from 95% ethanol and assayed for homogeneity by thin-layer chromatography and by high-pressure reversed-phase liquid chromatography. Wolfrom[6,7] described the trimer **3** through heptamer **7** members of this series; the physical properties (melting points and optical rotations) of our compounds were in reasonable agreement with those previously reported. Octamer **8** and nonamer **9** appear to have gone previously unreported and were fully characterized.

Mass Spectra. In order to firmly establish the structures of compounds **2–9**, we developed a mass spectrometry method for compounds of this type. Positive-ion liquid secondary ion mass spectrometry[9] (LSIMS) employing 3-nitrobenzyl alcohol saturated with potassium acetate as a sample matrix and cesium ion bombardment gave spectra typified by that shown for compound **9** (Figure 1). This sample matrix for LSIMS was superior to glycerol, which was previously employed in the fast atom bombardment of mannooligosaccharides,[10] as well as to sulfolane, 50:50 glycerol–sulfolane, 2,4-di-*tert*-amylphenol, and 3-mercapto-1,2-propanediol. The signal lasted several minutes, an ion adduct indicative of molecular weight was obtained for all oligomers, and no switching of ion sources was required for calibration of the mass spectrometer.

Our mass spectra are dominated by potassium cationization of the molecule, M. For example, a strong $(M + K)^+$ ion (m/z 2733.8) corresponds to the isotope peak in the molecular ion cluster of **9** containing only ^{12}C isotopes. The most abundant peak in the molecular ion cluster of

0024-9297/90/2223-3747$02.50/0

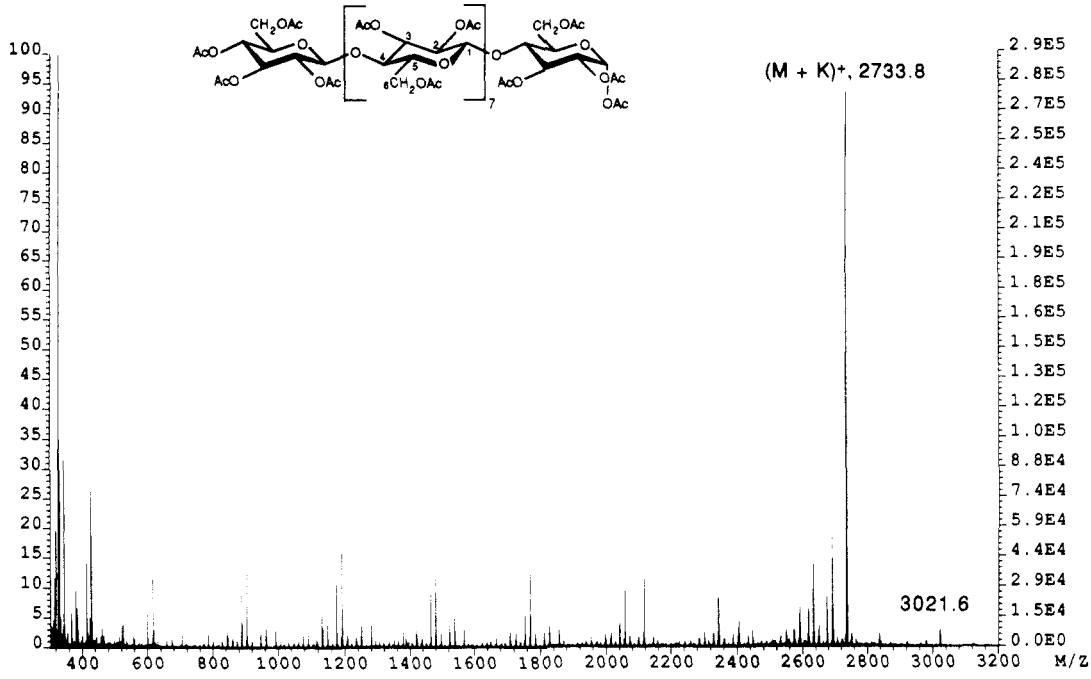

Figure 1. LSIMS spectrum of cellononaose nonacosaacetate (**9**) run in the presence of KOAc.

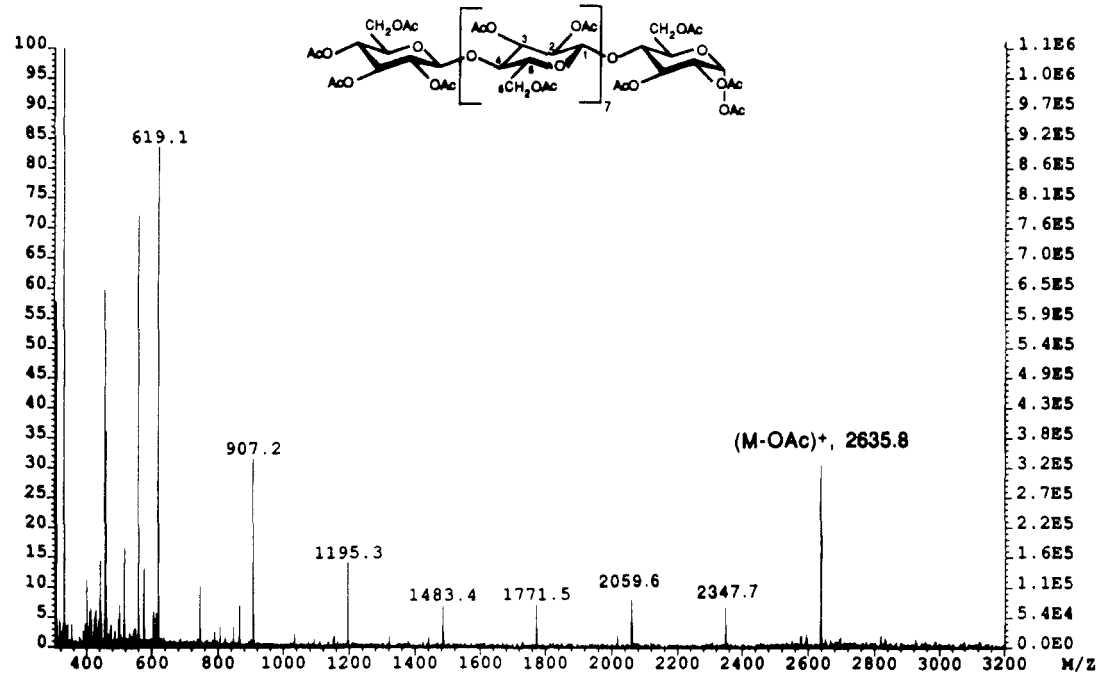

Figure 2. LSIMS spectrum of cellononaose nonacosaacetate (**9**) run in the absence of KOAc.

9 is 1 amu higher than the $(M + K)^+$ ion because the probability is higher for molecules of **9** containing one ^{13}C isotope and the remainder ^{12}C isotopes than for ones containing only ^{12}C isotopes. Several other ions are noted in the molecular ion region of the cationized molecules. Lower ions are a result of single or multiple loses of ketene and acetic acid fragments from the cationized molecular ion. A small $(M + K)^+$ ion at m/z 3021.6 disclosed the presence of a trace of decameric oligosaccharide. Another small $(M + K)^+$ ion at m/z 2836.3 discloses the presence of a trace of an acyclic byproduct previously identified in the acetolysis of other oligosaccharides.[10-12]

In the absence of potassium acetate in the sample matrix, spectra corresponding to Figure 2 were obtained. Ionization occurs with loss of the anomeric acetate to give a parent $(M - OAc)^+$ peak at m/z 2635.8. Subsequent fragmentations at each glycosidic linkage afford the observed series of ions. Analogous spectra were obtained for the series of compounds **2–8** and served to confirm the structures and purity of these substances.

LSIMS using 3-nitrobenzyl alcohol saturated with potassium acetate was the preferred method for obtaining mass spectra (vide supra). However, we also analyzed the samples by field desorption and ammonia chemical ionization mass spectrometry. Field desorption mass spectrometry gave spectra for **3–6** displaying $(M - OAc)^+$ ions similar to those obtained by LSIMS in the absence of potassium acetate. However, the higher oligomers **7–9** yielded no molecular weight information. The positive-ion (ammonia) chemical ionization mass spectrometry gave spectra displaying $(M + NH_4)^+$ ions for all samples

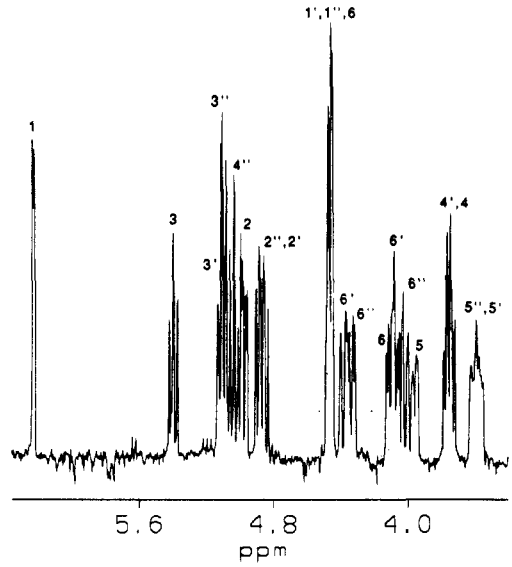

Figure 3. 1D ^{1}H NMR spectrum of the ring protons for cellotriose hendecaacetate (3).

examined. However, the signal response only lasted for ca. 10 s, and the instrument calibration had to be performed with the LSIMS ion source.

NMR Spectra. We have previously reported complete NMR spectral assignments and ^{13}C NMR T_1 values for CTA (1).[3-5] For the oligosaccharide series 2–9, we needed unambiguous assignments of all carbon atom resonances both for confirmation of structure and as a prerequisite to determination of ^{13}C NMR T_1 values. Through comparison to lower oligomers[13] and by using the normal variation in peak intensities for a series of homologous oligosaccharides, Capon et al.[14] have assigned the ring carbons of oligosaccharides 2–5. However, to our knowledge, assignments for the resonances of the ring carbons of oligosaccharides 6–9 have never been reported. Likewise, complete assignment of the ^{1}H NMR spectra and the carbonyl carbon resonances of oligosaccharides 2–9 has never been given.

In light of our requirements, we have used homonuclear correlated spectroscopy (COSY)[15] and the 2D version of the recently developed homonuclear Hartmann–Hahn (HOHAHA) method[16] for the assignment of the ^{1}H NMR spectra of 2–9. Because of the severe spectral overlap in the ^{1}H NMR spectra of 2–9, the 2D HOHAHA experiment proved to be especially useful in these spectral assignments. Assignment of the ring carbons was accomplished via the well-known one-bond heteronuclear correlation experiment (CHCOR).[17] Assignment of the carbonyl carbon resonances of 2 and 3 was accomplished by using a three-bond version of the heteronuclear correlation experiment.[18] For the higher oligomers 4–7, the three-bond CHCOR experiment proved to be too insensitive, and the carbonyl carbon resonances of these oligomers were assigned by using the one-dimensional experiment INAPT.[3,19] For oligomers 8 and 9, we found direct assignment of the carbonyl resonances unnecessary since the chemical shifts of the carbonyl resonances of the lower oligomers in this series of homologous oligosaccharides did not change with increasing DP. To demonstrate our approach, we outline the assignment of the ^{13}C and ^{1}H NMR resonances for cellotriose hendecaacetate (3).

Figure 3 shows the 1D ^{1}H NMR spectrum for the ring protons of 3. The resonance for H1 at 6.22 ppm serves as a label for the reducing end monomer, whereas the

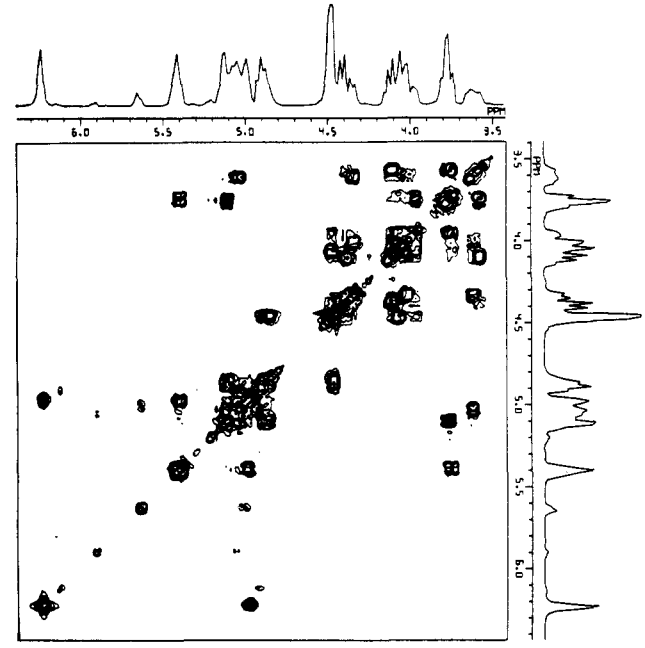

Figure 4. 2D COSY spectrum of cellotriose hendecaacetate (3).

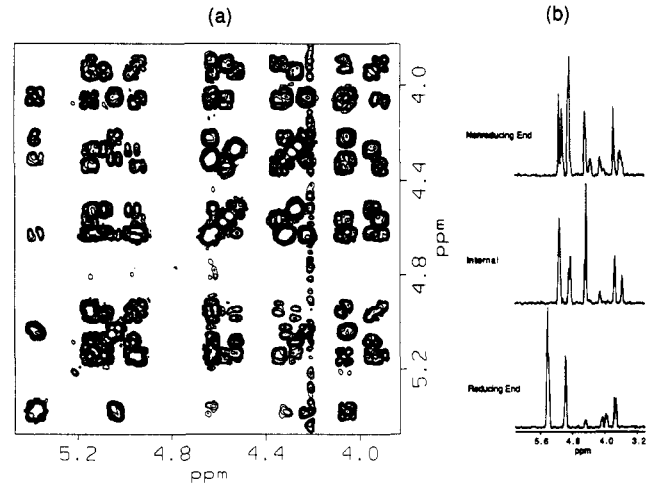

Figure 5. (a) 2D HOHAHA spectrum of cellotriose hendecaacetate (3). (b) Subspectra for each monomer obtained by taking slices through the F_1 dimension.

resonances for H4″ and H5″ at 5.02 and 3.60 ppm serve the same role for the nonreducing terminus.[3] Using these labels for the two terminal monomers, we can trace out their coupling networks by using the COSY and 2D HOHAHA spectra shown in Figures 4 and 5. The coupling network for the internal monomer is determined by default. Because of severe spectral overlap, complete assignment of the ^{1}H NMR spectrum of 3 would be difficult at best given only the COSY spectrum in Figure 4. However, the 2D HOHAHA NMR spectrum and the 1D subspectra, obtained by taking slices in the F_1 dimension of the 2D spectrum, greatly simplified the assignment of the resonances belonging to the coupling networks of both the internal and terminal residues. Given assignments for the ^{1}H NMR resonances of the reducing and nonreducing termini as well as for the internal monomer, the carbon resonances could be easily assigned via the one-bond and three-bond[18] heteronuclear experiments shown in Figure 6. The complete ^{1}H and ^{13}C NMR spectral assignments for 3 as well as for oligomers 2, 4–9, and for CTA (1) have been collected in Tables I–III.

As can be seen from the data in Tables I–III, the chemical shifts of the ring protons, the ring carbons, and,

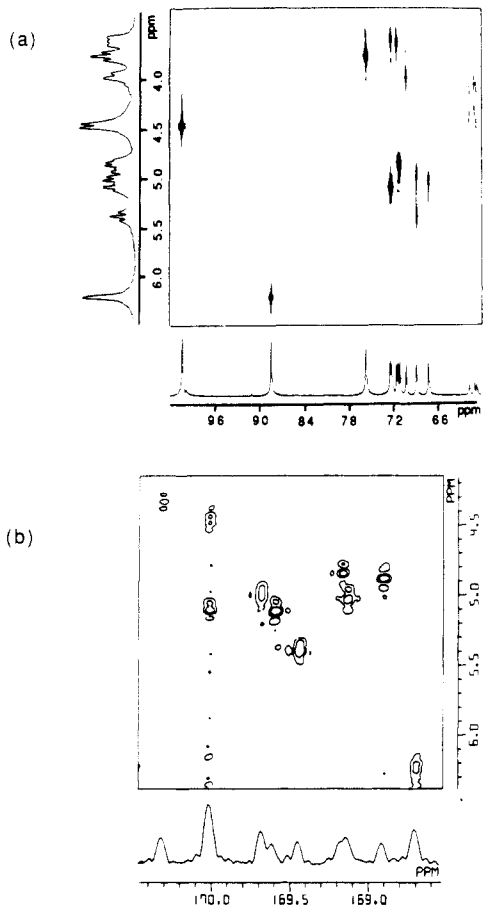

Figure 6. (a) One-bond and (b) three-bond 2D CHCOR spectra of cellotriose hendecaacetate (3).

in particular, the carbonyl carbons show little variation with increasing DP. By the time the heptamer is reached, both the carbon and the proton spectra (excluding end groups) have the basic features of the spectra of CTA (1) (Figure 7). Of particular interest are the chemical shifts of the C1's. Table II and Figure 7 both show that C1 resonances of the nonreducing end and of the internal residue of the triose 3 perfectly overlap. A C1 resonance for an oligosaccharide that overlaps with the C1 resonance of CTA (1) is first observed with the tetraose 4. For the pentaose 5 and the hexaose 6, four C1 resonances are observed in the 100–101 ppm region. When the heptamer 7 is reached, the resonance at 100.4 ppm begins to show the broadened appearance associated with the C1 of CTA (1). It is clear from the intensities of C1 peaks in Figure 7 that the downfield C1 (100.8 ppm) for 3–9 represents two monomers, one of which must be an internal residue whose C1 chemical shift is distinct from other internal residues. In contrast to Capon et al.,[14] we believe that the spectra are more consistent with this "special" residue being the glucose monomer adjacent to the nonreducing terminus. Nevertheless, it is apparent that a distribution of slightly differing C1 resonances is observable for oligomers 3–6 which must be accounted for in any molecular modeling program involving this family of oligosaccharides.

Spin Relaxation Times. The utility of ^{13}C NMR spin–lattice relaxation measurements in the study of the molecular motions of oligosaccharides and polysaccharides in solution has been well documented.[2,5,20] Tables IV and V give the T_1 relaxation times for oligosaccharides 2–9 as well as for CTA (1). The average T_1 values for the nonoverlapping reducing, nonreducing, and internal ring carbons are plotted versus DP in Figure 8. The T_1 values for the ring carbons of the respective monomers decrease in the order nonreducing > reducing > internal. The T_1 values for the reducing-end C1 are not included in the reducing-end monomer values since the former values appear to be unique. That is, the T_1 values for the reducing-end C1 are generally the least of any of the ring carbons, suggesting that the mobility of this carbon is the most restricted. Figure 8 also shows that the T_1 values of the internal ring carbons approach those for CTA (1) at a DP of ca. 7. A critical DP of 7 is consistent with the observed C1 chemical shifts (vide supra) and with the carbonyl carbon T_1 values illustrated in Figure 9.[21]

Differential Scanning Calorimetry. The melting points of compounds 2–9 were determined by DSC and open-capillary techniques and are shown in Table VI. T_m values between the two techniques agreed well with one another and literature values.[6,7] The measured T_m values increase in a monotonic fashion, with the exception of 2, leveling off at 260–265 °C for compounds 7–9. Heats of fusion (H_f) were also measured by DSC for compounds 2–9 and are included in Table VI. For the higher oligomers, the H_f appears to be leveling off at 4.5–5.0 kcal/mol of monomer.

The T_m of high molecular weight polymers can be estimated from the T_m of oligomers.[22,23] This approach, which has been applied to alkanes[22] and oxymethylene oligomers,[23] can be used to estimate the equilibrium melting point and heat of fusion for fully acetylated, high molecular weight CTA according to

$$1/T_m = 1/T_m^* + (2R/H_f)(1/n) \quad (1)$$

where T_m is the melting temperature of the oligomer with degree of polymerization n, T_m^* is the equilibrium melting point of the CTA with infinite chain length, H_f is the molar heat of fusion, and R is the universal gas constant. Thus a plot of $1/T_m$ against $1/n$ will provide $1/T_m^*$ and $2R/H_f$ as the intercept and slope, respectively. As shown in Figure 10 this plot is linear and gives a T_m^* of 294 °C and a H_f of 4.9 kcal/mol.

These values compare resonably well with the values reported for CTA (1). Malm[24] measured the T_m of CTA as 306 °C, and the work of Kamide[25] can be used to estimate a T_m of 305 °C. The H_f of CTA is difficult to measure as the polymer begins to degrade below its T_m.[25] Recognizing these difficulties, we measured a H_f for CTA of 4.6 kcal/mol in our laboratories from the melting point depression of CTA upon the addition of triaryl phosphate plasticizers. These values agree very well with those obtained from eq 1.

For compounds 3–9 the second-cycle DSC scans show a glass transition temperature (T_g) and cold crystallization exotherm (T_c) as well as a T_m (Table VI). The second-cycle DSC scans for several of the oligomers as well as CTA polymer are shown in Figure 11. The T_g of the oligomers is relatively well defined compared to that of the CTA polymer, while the T_c exotherms and T_m endotherms are similar for both the oligomers and polymer. The H_f for the second-cycle T_m is lower than for the first, indicating a reduction in the degree of crystallinity of the thermally crystallized materials. This is consistent with the thermal behavior of many cellulose esters and shows that the degree of crystallinity is strongly dependent on the mode of crystallization.

The T_g is known to be dependent on molecular weight, and this dependence has been modeled several ways.[26,27] Over a wide molecular weight range this relationship has been shown to be nonlinear.[27] However, over a narrow molecular weight range a simple linear approach can be

Table I
^{1}H NMR Chemical Shifts (δ) for Oligosaccharide Peracetates 2–9 and for CTA (1)

monomer(s)	2	3	4	5	6	7	8	9	1[a]
reducing									
H1	6.23	6.22	6.21	6.22	6.22	6.22	6.22	6.22	
H2	4.99	4.97	4.96	4.97	4.97	4.97	4.97	4.96	
H3	5.42	5.38	5.38	5.39	5.39	5.39	5.39	5.39	
H4	3.77	3.74	3.72	3.73	3.72	3.71	3.70	3.70	
H5	3.97	3.95	3.95	3.95	3.95	3.95	3.95	3.95	
H6	4.46	4.45	4.45	4.45	4.45	4.45	4.45	4.45	
	4.09	4.06	4.04	4.08	4.05	4.05	4.05	4.05	
internal[b]									
H1		4.45 (4.46)	4.41 (4.44)	4.40 (4.44)	4.40 (4.44)	4.40 (4.44)	4.40 (4.44)	4.39 (4.44)	4.42
H2		4.85	4.82 (4.79)	4.80 (4.78)	4.79	4.78	4.78	4.78	4.79
H3		5.10	5.08 (5.07)	5.07 (5.06)	5.07	5.07	5.07	5.07	5.07
H4		3.76	3.72	3.73 (3.71)	3.72	3.71	3.69 (3.73)	3.69 (3.73)	3.71
H5		3.56	3.55	3.55 (3.52)	3.54	3.54	3.53	3.53	3.53
H6		4.38	4.36	4.37	4.37	4.36	4.36	4.36	4.36
		4.10	4.07	4.08 (4.05)	4.05	4.05	4.05	4.05	4.06
nonreducing									
H1	4.49	4.45	4.44	4.44	4.44	4.44	4.44	4.44	
H2	4.93	4.88	4.89	4.86	4.88	4.87	4.87	4.87	
H3	5.13	5.10	5.09	5.09	5.10	5.10	5.11	5.10	
H4	5.06	5.03	5.02	5.03	5.02	5.02	5.02	5.03	
H5	3.64	3.60	3.60	3.60	3.60	3.60	3.60	3.60	
H6	4.37	4.33	4.32	4.33	4.33	4.33	4.32	4.33	
	4.02	4.01	4.00	4.00	4.00	4.00	4.00	4.00	

[a] Taken from ref 4. [b] Resonances for additional, nonoverlapping internal protons are given in parentheses. No attempt was made to distinguish between internal residues.

Table II
^{13}C NMR Chemical Shifts (δ) for the Ring Carbons of Oligosaccharide Peracetates 2–9 and for CTA (1)

monomer(s)	2	3	4	5	6	7	8	9	1[a]
reducing									
C1	88.9	88.9	88.9	88.9	88.9	88.9	88.9	88.9	
C2	69.3	69.4	69.3	69.3	69.3	69.4	69.4	69.3	
C3	69.3	69.4	69.3	69.3	69.3	69.4	69.4	69.3	
C4	76.0	76.0	76.0	76.0	76.0	76.0	76.0	76.0	
C5	70.7	70.7	70.7	70.7	70.7	70.8	70.7	70.7	
C6	61.3	61.2	61.2	61.2	61.2	61.3	61.3		
internal[b]									
C1		c	100.4	100.4 (100.5)	100.4 (100.5)	100.4	100.4	100.4	100.4
C2		71.8	71.9 (71.7)	71.9 (71.8)	71.9	71.9 (71.8)	71.9	71.9	71.7
C3		72.7	72.6	72.6 (72.5)	72.5	72.5 (72.6)	72.5	72.5	72.5
C4		76.1	76.1	76.0	76.0	76.0	76.0	76.0	76.0
C5		72.8	72.8	72.8	72.8	72.8	72.8	72.8	72.7
C6		62.2	62.1 (62.0)	62.0	62.0	62.0 (62.2)	62.0 (62.3)	62.0	61.9
nonreducing									
C1	100.8	100.7	100.7	100.7	100.7	100.7	100.7	100.7	
C2	71.6	71.6	71.5	71.6	71.6	71.6	71.6	71.6	
C3	72.9	72.9	72.7	72.8	72.8	72.8	72.8	72.8	
C4	67.8	67.8	67.7	67.8	67.8	67.8	67.8	67.8	
C5	72.0	72.0	72.0	72.0	72.0	72.0	71.9	71.9	
C6	61.6	61.5	61.5	61.5	61.5	61.5	61.5	61.5	

[a] Taken from ref 4. [b] Resonances for additional, nonoverlapping internal carbons are given in parentheses. No attempt was made to distinguish between internal residues. [c] C1 of the middle monomer of 3 is indistinguishable from the nonreducing end. See the text for details.

used to model the T_g–molecular weight dependence:[26]

$$T_g = T_g^* - k/M_n \quad (2)$$

where T_g is the measured glass transition temperature, T_g^* is the glass transition temperature for the high molecular weight polymer, k is a constant, and M_n is the number-average molecular weight. Using this relationship, we calculated the T_g^* from the second-cycle T_g of the oligomers (Figure 12). This T_g^* was 160 °C, which is lower than the 175 °C measured in our laboratories for true CTA and the 189 °C estimated by Kamide.[25] For low molecular weight oligomers, the linear T_g–M_n relationship is expected to predict a T_g below that seen for the high molecular weight polymer.[27]

Conclusion

The series of cellooligosaccharide acetates 2–9 has been fully characterized by NMR and mass spectrometry. In addition, we report a number of other physical properties for this series, including heat of fusion, T_m, and T_g.

The results from the NMR spectroscopy study show that for this series of oligosaccharides, the critical degree of polymerization is reached at ca. 7. A critical DP of 7, nearly half of that found by Benesi and Brant[2] for pullulan, demonstrates the higher chain rigidity of this series of cellooligosaccharides relative to the maltooligosaccharide series. In addition, the NMR spectroscopy data show that a distribution of chemical shift environments exists for C1's in the lower oligomers and that the termini of these oli-

Table III
^{13}C NMR Chemical Shifts (δ) for the Carbonyl Carbons of Oligosaccharide Peracetates 2–9 and for CTA (1)

monomer(s)	2	3	4	5	6	7	8	9	1[a]
reducing									
C1Ac	168.7	168.7	168.7	168.7	168.7	168.7	168.7	168.7	
C2Ac	169.7	169.7	169.7	169.7	169.7	169.7	169.6	169.6	
C3Ac	169.5	169.5	169.5	169.5	169.5	169.5	169.6	169.6	
C6Ac	170.1	170.0	170.0	170.1	170.1	170.1	170.1	170.1	
internal									
C2Ac		169.2	169.2	169.2	169.2	169.2	169.2	169.2	169.2
C3Ac		169.6	169.6	169.6	169.6	169.6	169.6	169.6	169.6
C6Ac		170.0	170.1	170.1	170.1	170.1	170.1	170.1	170.1
nonreducing									
C2Ac	168.9	168.9	169.0	168.9	169.0	169.0	169.0	168.9	
C3Ac	170.0	170.0	170.0	170.1	170.1	170.1	170.1	170.1	
C4Ac	169.2	169.2	169.2	169.2	169.2	169.2	169.2	169.2	
C6Ac	170.3	170.3	170.4	170.3	170.3	170.3	170.3	170.3	

[a] Taken from ref 4.

Table IV
^{13}C NMR T_1 (s) Times for the Ring Carbons of Oligosaccharide Peracetates 2–9 and for CTA (1)

monomer(s)	2	3	4	5	6	7	8	9	1[a]
reducing									
C1	0.39	0.26	0.22	0.20	0.20	0.19	*b*	*b*	
C2	0.44	0.31	0.27	0.25	0.25	0.23	0.22	0.22	
C3	0.44	0.31	*b*	0.25	0.25	0.23	0.22	0.22	
C4	0.45	0.29	0.25	0.22	0.20	0.20	0.19	0.18	
C5	0.44	0.30	0.27	0.24	0.26	0.25	0.23	*b*	
C6	0.47	0.32	0.28	*b*	*b*	0.26	0.25	*b*	
internal[c]									
C1		*d*	0.25	0.23	0.20	0.21	0.20	0.20	0.20
C2		0.29	0.25	0.24	0.21	0.20	0.19	0.18	0.21
C3		0.30	0.25	0.22	0.21	0.21	0.20	0.19	0.20
C4		0.29	0.25	0.22	0.20	0.20	0.19	0.18	0.20
C5		0.29	0.25	0.23	0.21	0.21	0.19	0.19	0.20
C6		0.30	0.25	*b*	*b*	0.21	0.18	0.18	0.20
nonreducing									
C1	0.46	0.31	0.26	0.24	0.25	0.26	0.22	0.23	
C2	0.43	0.31	0.27	0.25	0.26	0.24	0.24	0.20	
C3	0.45	0.32	0.25	0.23	0.21	0.21	0.19	0.19	
C4	0.43	0.33	0.26	0.28	0.27	0.30	0.28	0.21	
C5	0.43	0.33	0.28	0.22	0.24	0.23	0.19	0.18	
C6	0.52	0.36	0.34	*b*	0.24	0.26	0.32	0.36	

[a] Taken from ref 5. [b] These values were not obtained due to a low signal-to-noise ratio and insufficient points. [c] When more than one internal monomer resonance could be identified for a carbon, the values were averaged. [d] C1 of the middle monomer of 3 is indistinguishable from the nonreducing end. See text for details.

gosaccharides must be viewed as consisting of three residues: one reducing monomer, one nonreducing monomer, and the anhydroglucose monomer adjacent to the nonreducing terminus.

The DSC data demonstrate that the thermal properties of compounds **2–9** can be used to estimate the T_g, T_m, and H_f of fully acetylated, high molecular weight CTA. These results are particularly valuable since the T_m and H_f are otherwise uncertain due to thermal decomposition of the polymer. The agreement between the estimated and actual values was quite good, indicating that the oligomer series could be used to estimate many of the properties of the high molecular weight polymer.

Experimental Section

Materials. Cellulose triacetate (1) was prepared as previously described.[4] α-D-Cellobiose octaacetate (2) was used as obtained from Aldrich Chemical Co. Compounds **3–9** were prepared according to the general methods of Wolfrom and co-workers;[6-8] compounds **6–9** were obtained from V-Labs, Inc.[28] The compounds were twice recrystallized from 95% ethanol and dried in vacuo at ca. 60 °C. Product homogeneity was established by HPLC analysis on a 1-dm C18 reversed-phase column eluted with a linear program from 50:50 to 90:10 acetonitrile–water; detection was by UV at 220 nm. Optical rotations were run in $CHCl_3$ at sample concentrations of 4–11 mg/mL on a Rudolf Autopol III instrument. Molar quantities are expressed in terms of moles of peracetylated monomer.

α-D-Cellotriose hendecaacetate (3): mp (capillary, uncorr) 214–217 °C (lit.[6] mp 223–224, 219–220 °C); LSIMS m/z 1005.3 (calcd for $(M + K)^+$, 1005.3); $[\alpha]^{20}_D$ +18.4° (lit.[6] $[\alpha]^{20}_D$ +22.4°).

α-D-Cellotetraose tetradecaacetate (4): mp 221–224 °C (lit.[6] mp 230–234 °C); LSIMS m/z 1293.5 (calcd for $(M + K)^+$ 1293.3); $[\alpha]^{20}_D$ +12.8° (lit.[6] $[\alpha]^{20}_D$ +13.4°).

α-D-Cellopentaose heptadecaacetate (5): mp 234–238 °C (lit.[6] mp 240–241 °C); LSIMS m/z 1581.6 (calcd for $(M + K)^+$ 1581.4); $[\alpha]^{20}_D$ +4.85° (lit.[7] $[\alpha]^{20}_D$ +4.7°).

α-D-Cellohexaose eicosaacetate (6): mp 251–256 °C (lit.[7] mp 252–255 °C); LSIMS m/z 1869.6 (calcd for $(M + K)^+$, 1869.5); $[\alpha]^{20}_D$ −0.67° (lit.[7] $[\alpha]^{20}_D$ −0.23°).

α-D-Celloheptaose tricosaacetate (7): mp 259–261 °C (lit.[7] mp 263–266 °C); LSIMS m/z 2157.5 (calcd for $(M + K)^+$ 2157.6); $[\alpha]^{20}_D$ −3.79° (lit.[7] $[\alpha]^{20}_D$ −4.4°).

α-D-Cellooctaose hexacosaacetate (8): mp 258–262 °C; LSIMS m/z 2445.7 (calcd for $(M + K)^+$, 2445.7); $[\alpha]^{20}_D$ −4.82°.

α-D-Cellononaose nonacosaacetate (9): mp 258–263 °C; LSIMS m/z 2733.8 (calcd for $(M + K)^+$, 2733.8); $[\alpha]^{20}_D$ −6.77°.

Table V
^{13}C NMR T_1 (s) Times for the Carbonyl Carbons of Oligosaccharide Peracetates 2–9 and for CTA (1)

monomer(s)	2	3	4	5	6	7[a]	8	9	1[b]
reducing									
C1Ac	5.9	4.2	3.9	2.8	3.4	3.4	3.1	3.5	
C2Ac	5.8	4.1	3.5	2.8	2.6	2.5	1.8	1.9	
C3Ac	6.3	3.8	3.6	2.5	2.8	3.0	1.8	1.9	
C6Ac	6.9	4.4	3.6	3.2	3.0	3.1	2.5	2.7	
internal									
C2Ac		3.6	3.1	2.5	2.4	2.3	1.9	2.0	2.3
C3Ac		3.4	2.9	2.5	2.2	2.2	1.8	1.9	2.0
C6Ac		4.4	4.2	3.2	3.0	3.1	2.5	2.7	2.5
nonreducing									
C2Ac	5.1	3.8	3.2	2.6	2.5	3.3	2.6	2.6	
C3Ac	6.6	4.4	3.6	3.2	3.0	3.1	2.5	2.7	
C4Ac	5.9	3.7	3.1	2.4	2.4	2.3	1.9	2.0	
C6Ac	8.1	6.0	6.1	4.1	4.6	4.7	3.3	3.7	

[a] The carbonyl T_1 values for 7 exhibited the greatest variance in multiple experiments. These values are the average from four sets of experiments. The deviation for the carbonyl carbons of the terminal monomers ranged from 12 to 21%. The deviation for the carbonyl carbons of the internal monomers ranged from 8 to 10%. [b] Taken from ref 5.

Table VI
Capillary Melting Points and DSC Data for Oligosaccharide Peracetates 2–9 and for CTA (1)

oligomer	capillary T_m, °C	lit. T_m,[6,7] °C	T_m,[a] °C	H_f, kcal/mol	T_m,[b] °C	T_g,[b] °C	T_c,[b] °C
glu(OAc)$_5$	105–109	105–108	112	5.5	112		90
2	223–227	225–226	226	6.8	224		108[c]
3	214–216	223–224	218	3.6	217	92	150
4	228–231	230–234	227	3.8	226	100	176
5	234–238	240–244	240	2.1	240	107	199
6	248–252	252–255	256	4.1	254	123	195
7	259–261	263–266	265	4.6	258	123	190
8	258–262		262			132	
9	258–262		264		251[c]	136	178
CTA			306	1.7	297	156	189

[a] First-cycle DSC scan. [b] Second-cycle DSC scans. [c] Two peaks were observed in the DSC spectrum.

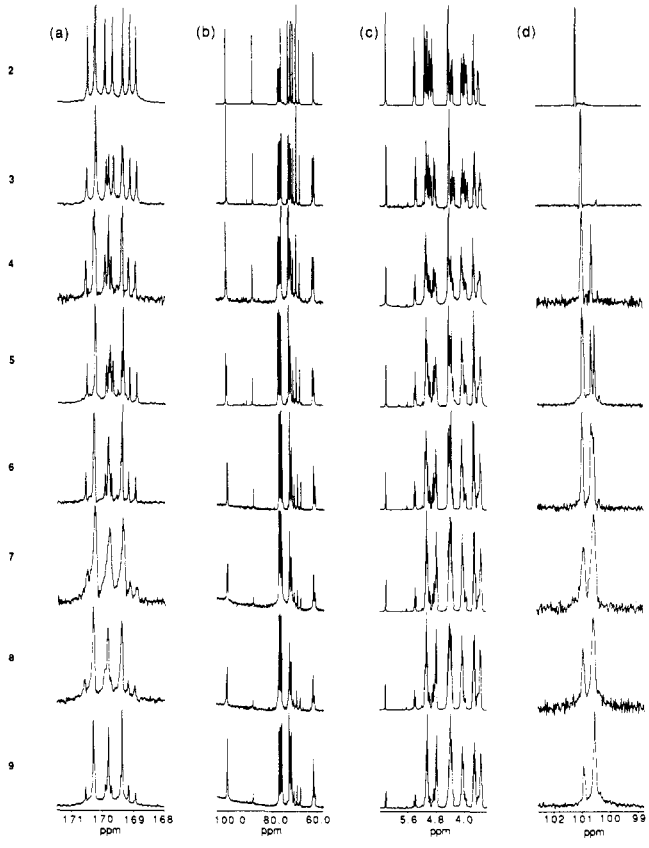

Figure 7. Resonances for (a) carbonyl carbons, (b) ring carbons, (c) ring protons, and (d) C1 carbons for 2–9. Mild resolution enhancement[4] has been applied to each spectrum.

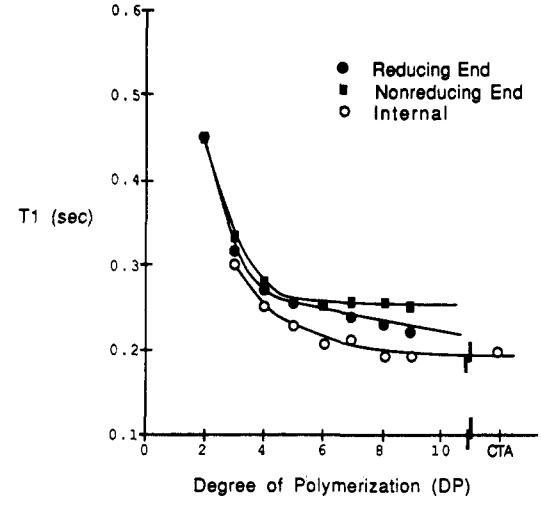

Figure 8. Plot of ring-carbon T_1 values versus degree of polymerization for 1–9.

Mass Spectra. Mass spectra of 3–9 were obtained on a Vacuum Generators VG 7070SEQ mass spectrometer equipped with a VG cesium ion gun operated at 35 keV. The instrument was scanned from 3300 to 300 amu in 5 s with an interscan delay time of 1 s at a resolution of ca. 3000. The spectrometer was calibrated with cesium iodide. Samples were prepared by wetting the LSIMS probe tip with 3-nitrobenzyl alcohol saturated with potassium acetate. The saturated solution of potassium acetate in 3-nitrobenzyl alcohol was prepared by heating a mixture of 70 mg of potassium acetate with 1600 mg of 3-nitrobenzyl alcohol. The tip of a plunger from a 10-μL Hamilton syringe was wet with 3-nitrobenzyl alcohol and used to transfer 50–100 μg of the oligosaccharide to the LSIMS probe. About 15 s was required for

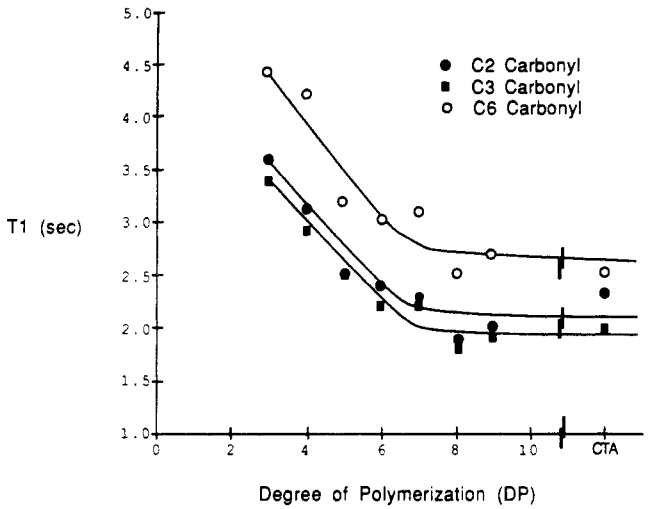

Figure 9. Plot of internal carbonyl carbon T_1 values versus degree of polymerization for 1 and 3–9.

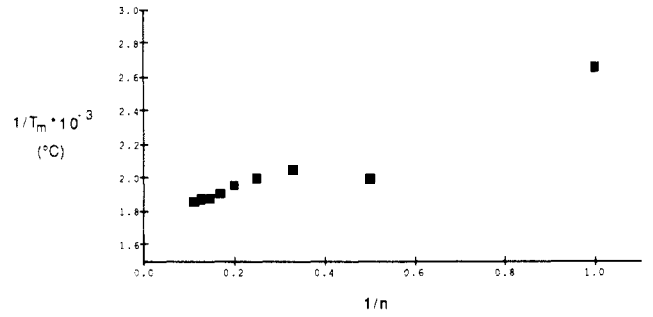

Figure 10. Plot of $1/T_m$ versus $1/n$ for peracetylated glucose and for 2–9.

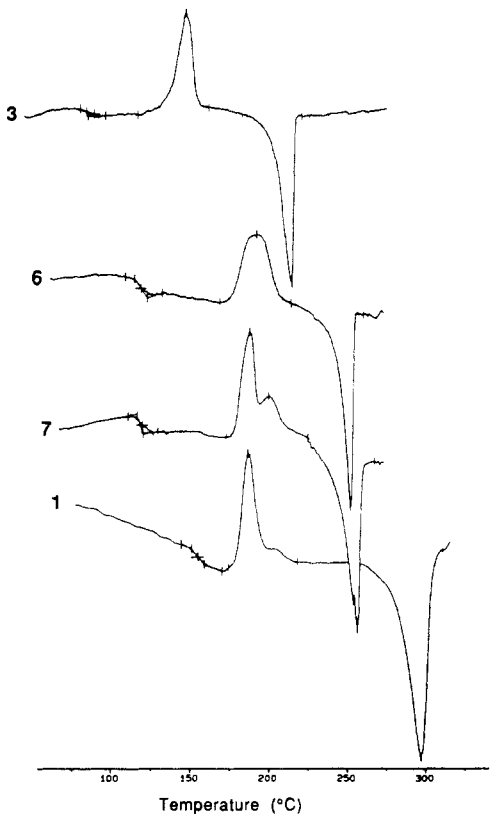

Figure 11. Second-cycle DSC scans for 1, 3, 6, and 7.

the signal strength to reach maximum after switching on the ion beam; 10–30 scans were averaged to obtain the spectra. Spectra of 8 and 9 were also obtained in the absence of potassium acetate and showed fragmentation patterns as in Figure 2. Mass spectra

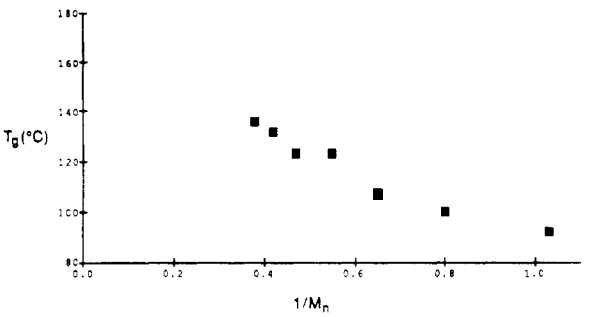

Figure 12. Plot of T_g versus $1/M_n$ for 3–9.

of 3 and 9 dissolved in methylene chloride were obtained by direct chemical ionization employing ammonia as the reagent gas. Mass spectra of lower oligomers 3–6, dissolved in methylene chloride, were obtained on a VG ZAB mass spectrometer operated in the field desorption mode.

NMR Spectra. Proton NMR data were obtained on a JEOL Model GX-400 NMR spectrometer operating at 400 MHz. The sample tube size was 5 mm, and the sample concentrations were ca. 10 mg/mL of $CDCl_3$.

Carbon-13 NMR data were obtained on a JEOL Model GX-270 NMR spectrometer operating at 67.9 MHz. The sample tube size was 10 mm, and the sample concentrations were 0.35 M in $CDCl_3$ (moles per liter of sugar residue) in all cases. The samples were degassed by using the freeze–pump–thaw technique before sealing the tube under an argon atmosphere.

Chemical shifts are reported in ppm from tetramethylsilane, with $CHCl_3$ as an internal reference. For ^1H NMR spectra, residual $CHCl_3$ was taken as 7.24 ppm. For ^{13}C NMR spectra, the center peak of the triplet resonance of $CDCl_3$ was taken as 77.0 ppm.

The COSY spectrum shown in Figure 4 was collected by using a 512 × 1024 data matrix size, and 64 transients were acquired for each t_1 value. The spectrum was processed by using a sine bell filtering function in both dimensions. The delay time between scans was 1.6 s, and the total measuring time was 17 h.

The 2D HOHAHA spectrum shown in Figure 5 is the result of a 512 × 1024 data matrix zero-filled to a 1024 × 1024 matrix, with 16 scans per t_1. A pulse delay of 1.0 s was used between scans, and the total measuring time was 14 h. An MLEV-17 sequence of 54 ms and two 2.5-ms trim pulses was used.[16b] The HOHAHA data were processed with a Macintosh computer, with VersaTerm Pro (Version 3.0) as an emulation package, on a VAX 8800 using FTNMR software.[29]

The one-bond heteronuclear chemical shift correlation spectrum shown in Figure 6 was recorded by using a 512 × 2048 data matrix size and 96 scans for each t_1 value. The values for Δ^1 and Δ^2 were 3.0 and 2.2 ms. The total measuring time was 24 h.

The three-bond heteronuclear chemical shift correlation spectrum, also shown in Figure 6, is the result of a 64 × 128 data matrix zero-filled to 512 × 1024, with 448 scans for each t_1 value. The values for Δ_1 and Δ_2 were 70.0 and 100.0 ms. The total measuring time was 44 h.

The inversion–recovery method with complete decoupling of protons was used to collect spin–lattice relaxation times (T_1). The carbonyl and ring carbon T_1 values were collected separately. For the ring carbons, the frequency window was 3287 Hz, the pulse delay was 4 s, and 512–1024 scans were used to collect each spectrum. For the carbonyl carbons, the frequency window was 439 Hz, the pulse delay was 15 s, and 256–640 scans were used to collect each spectrum. All of the T_1 measurements were made at 33 °C. For the ring carbons, the experimental T_1 values were multiplied by the number of attached protons.

DSC. The differential scanning calorimetry (DSC) scans were obtained on a Perkin-Elmer DSC 2 equipped with a TADS computer. Samples of 4–6 mg were run under nitrogen at 20 °C/min for the heating scans and 20 °C/min for the cooling cycle. DSC calibration was done with indium and lead.

Acknowledgment. We thank Eddie Forbes and Dr. Douglas W. Lowman for their technical support and helpful comments.

References and Notes

(1) (a) Kennedy, J. F.; Phillips, G. O.; Williams, P. A. *Wood and Cellulosics: Industrial Utilization, Biotechnology, Structure and Properties*; Ellis Horwood: Chichester, 1987. (b) Kennedy, J. F.; Phillips, G. O.; Wedlock, D. J.; Williams, P. A. *Cellulose and Its Derivatives: Chemistry, Biochemistry, and Applications*; Ellis Horwood: Chichester, 1985. (c) Nevell, T. P.; Zeronian, S. H. *Cellulose Chemistry and Its Applications*; Ellis Horwood: Chichester, 1985.
(2) Benesi, A. J.; Brant, D. A. *Macromolecules* **1985**, *18*, 1109.
(3) Buchanan, C. M.; Hyatt, J. A.; Lowman, D. W. *Carbohydr. Res.* **1988**, *177*, 228.
(4) Buchanan, C. M.; Hyatt, J. A.; Lowman, D. W. *Macromolecules* **1987**, *20*, 2750.
(5) Buchanan, C. M.; Hyatt, J. A.; Lowman, D. W. *J. Am. Chem. Soc.* **1989**, *111*, 7312.
(6) Dickey, E. E.; Wolfrom, M. L. *J. Am. Chem. Soc.* **1949**, *71*, 825.
(7) Wolfrom, M. L.; Dacons, J. C. *J. Am. Chem. Soc.* **1952**, *74*, 5331.
(8) Wolfrom, M. L.; Dacons, J. C.; Fields, D. L. *Tappi* **1956**, *39*, 803.
(9) Aberth, W. A.; Burlingame, A. L. *Anal. Chem.* **1984**, *56*, 2915.
(10) Tsai, P.-K.; Dell, A.; Ballou, C. E. *Biochemistry* **1986**, *82*, 4119.
(11) Lindberg, B. *Acta Chem. Scand.* **1949**, *3*, 1350.
(12) This acyclic byproduct was not detected by HPLC, TLC, ^{1}H NMR, or ^{13}C NMR and, hence, must be present in trace amounts or its presence is obscured by peak overlap.
(13) Gagnaire, D. Y.; Taravel, F. R.; Vignon, M. R. *Carbohydr. Res.* **1976**, *51*, 157.
(14) Capon, B.; Rycroft, D. S.; Thompson, J. W. *Carbohydr. Res.* **1979**, *70*, 145.
(15) (a) Nagayama, K.; Kumar, A.; Wuthrich, K.; Ernst, R. R. *J. Magn. Reson.* **1980**, *40*, 321. (b) Bax, A.; Freeman, R. *J. Magn. Reson.* **1981**, *44*, 542.
(16) (a) Bax, A.; Davis, D. G. *J. Am. Chem. Soc.* **1985**, *107*, 2820. (b) Bax, A.; Davis, D. G. *J. Magn. Reson.* **1985**, *65*, 355. (c) Summers, M. F.; Marzilli, L. G.; Bax, A. *J. Am. Chem. Soc.* **1986**, *108*, 4285.
(17) (a) Maudsley, A. A.; Muller, L.; Ernst, R. R. *J. Magn. Reson.* **1977**, *28*, 463. (b) Bax, A.; Morris, G. A. *J. Magn. Reson.* **1981**, *42*, 501.
(18) Goux, W. J.; Unkefer, C. J. *Carbohydr. Res.* **1987**, *159*, 191.
(19) Bax, A. *J. Magn. Reson.* **1984**, *57*, 314.
(20) (a) Benesi, A. J.; Gerig, J. T. *Carbohydr. Res.* **1977**, *53*, 278. (b) Matsuo, K. *Macromolecules* **1984**, *17*, 449.
(21) As is evident from Table III, overlap among the carbonyl resonances is unavoidably present. Nevertheless, it is gratifying that the T_1 values for the carbonyl carbons also suggest a critical DP of 7.
(22) Flory, P. J.; Vrij, A. *J. Am. Chem. Soc.* **1963**, *85*, 3548.
(23) Schmidt, G.; Enkelmann, V.; Westphal, U.; Droscher, M.; Wegner, G. *Colloid Polym. Sci.* **1985**, *263*, 120.
(24) Malm, C. J.; Mench, J. W.; Kendall, D. L.; Hiatt, G. D. *Ind. Eng. Chem.* **1951**, *43*, 688.
(25) Kamide, K.; Saito, M. *Polym. J.* **1985**, *17*, 919.
(26) (a) Fox, T. G.; Flory, P. J. *J. Appl. Phys.* **1950**, *21*, 581. (b) Fox, T. G.; Flory, P. J. *J. Polym. Sci.* **1954**, *14*, 315.
(27) Lee, C.-H.; Williams, M. C. *J. Macromol. Sci.—Phys.* **1987**, *B26*, 145.
(28) V-Labs, Inc., 423 North Theard St., Covington, LA 70433.
(29) Hare Research Inc., 14810 216th Av. N.E., Woodinville, WA 98072.

Poly(4-vinylpyridine) Complexes with Bromine and Bromine Chloride as Reactive Polymers in Addition Reactions

Jacob Zabicky* and Moshe Mhasalkar

The Institutes for Applied Research, Ben-Gurion University of the Negev, P.O. Box 1025, Beer Sheva 84110, Israel

Ida Oren

Department of Biophysics, The Weizmann Institute of Science, Rehovot, Israel

Received September 22, 1989; Revised Manuscript Received February 9, 1990

ABSTRACT: The following general features of poly(4-vinylpyridine)–halogen complexes (PVP–XY; X = Br, Y = Br, Cl) were observed, when reacting with olefinic and acetylenic compounds, as compared with the free halogens under similar conditions of solvent and temperature: reactions took place at much slower rates, allowing in most cases mixing of the total amounts of reacting materials in the reactor; when inert solvents were used, the isolated crude adducts were nearly pure compounds; with PVP–BrCl only small amounts of dibromo or dichloro adducts were formed; side reactions frequently accompanying additions of free halogens to double and triple bonds, such as HBr evolution, were absent. When addition to double bonds was carried out in a reactive solvent such as acetic acid, one-fourth to one-third of the product was a bromo–acetate adduct, while addition to acetylenic compounds gave no such byproducts. After the halogen of the polymeric reagent was consumed, the polymer could be filtered and regenerated for reuse. PVP–XY undergoes quaternization reactions concurrently with halogen addition to double or triple bonds. Such reactions may also lead to further cross-linking of the PVP network. Analogous quaternizations using monomeric pyridine–halogen reagents and acetylenic substrates point to various possible quaternization paths of the polymeric reagent: N-vinylation of one pyridyl group, attachment of two *N*-pyridyl groups at the 1,2-positions of a vinylidene group, or further transformations of the quaternary compounds, depending on the nature of the acetylenic substrate.

Introduction

The development of polymeric reagents has become an important branch of modern chemistry. Some reviews relevant to our subject have appeared.[1-3] Reactive polymers have been investigated in various halogenation processes in the past. The polymeric analogues of *N*-chloro- and *N*-bromoamides behaved similarly to or differently from the monomeric reagent, depending on the

0024-9297/90/2223-3755$02.50/0